Excess-substrate inhibition in enzymology and high-dose inhibition in pharmacology: a re-interpretation

Peter W. KÜHL
Institute of Theoretical Biology, Schaulistr. 2, CH-4142 Münchenstein BL, Switzerland

A kinetic model, called the Recovery Model, which incorporates an obligatory recovery phase of fixed duration (t_r) in the operation cycle of a macromolecule (enzyme, receptor) is proposed. Binding of a ligand (substrate, agonist) during t_r disturbs the recovery process and causes inhibition (substrate inhibition, agonist autoinhibition). A quantitative stochastic analysis of a minimal version of the Recovery Model reveals that (1) plotting the response versus the logarithm of the ligand concentration never yields a strictly symmetrical bell-shaped dose–response curve, (2) the position and shape of the descent of the dose–response curve can vary greatly in dependence of the kinetic parameters of the system, and (3) a minimal steepness of the descent with a Hill coefficient of 1 exists provided that the response can be totally inhibited by high ligand concentrations. The Recovery Model is equally applicable to macromolecules that can bind single or multiple ligands, and suggests new ways to explain such diverse phenomena as partial agonism, pulse generation, desensitization, memory effects and ultrasensitivity. In addition, substrate inhibition and agonist autoinhibition are regarded as phenomena closely related to other kinds of non-Michaelian behaviour because of a common temporal mechanism, namely the temporal interference of arriving ligand molecules with timing-sensitive phases of the operation cycle.

INTRODUCTION

Inhibition of enzymes by excess substrate concentrations, briefly called substrate inhibition, is one of the most common deviations from Michaelis–Menten kinetics and one of the best documented facts in enzymology. Since the first reports in the 19th century, substrate inhibition has been reported in thousands of publications and in all enzyme classes (EC 1 to EC 6), but, although recognized early on as an 'almost universal phenomenon' [1], it has nevertheless met an almost universal disinterest. Accordingly, there exist only few articles and reviews exclusively devoted to the theoretical treatment of substrate inhibition, and, in some monographs on enzyme kinetics, substrate inhibition is not even mentioned. Probably the main reason for this neglect is that the majority of enzymologists and many authorities in the field regard substrate inhibition as being almost always a non-physiological phenomenon. We doubt that substrate inhibition is of physiological significance in rare cases only, but even if it were so, we claim that a theoretical analysis of substrate inhibition, irrespective of whether it occurs under physiological or non-physiological conditions, can provide important clues for understanding the functioning of enzymes.

In the present paper we do not intend to give a comprehensive description of the complex phenomenology of substrate inhibition nor do we present a full account of the various mechanisms proposed previously for its explanation. We also do not treat the question of the physiological significance of substrate inhibition; rather we confine ourselves to proposing and discussing a new model for explaining substrate inhibition, termed by us the Recovery Model. This model postulates that, after the catalytic act, there occurs an obligatory recovery phase before a new operation cycle can start and that, as an approximation, the recovery phase is of fixed duration. Binding of a substrate molecule during the recovery phase gives rise to substrate inhibition. The Recovery Model is applicable not only to enzyme/substrate but also to receptor/agonist systems. In the latter systems it is well known that, analogously to substrate inhibition, high ('supramaximal') concentrations of an agonist (hormone, neurotransmitter, drug) often inhibit the response that low concentrations of the same agonist elicit or augment. This phenomenon has been given various names in the pharmacological literature, e.g. high-dose inhibition, autoinhibition, autoantagonism, autodesensitization, self-blockade, Arndt–Schulz law or Arndt–Schulz rule. Common to both phenomena, i.e. substrate inhibition in enzymology and high-dose inhibition in pharmacology [in the following collectively called high-ligand inhibition (HLI)], is a bell-shaped dose–response curve. [We here apply the term 'dose–response curve', commonly used only in pharmacology and physiology, to enzymes, and understand it to be a plot of the response versus the logarithm of the ligand concentration. The attribute 'bell-shaped' does not necessarily imply that the dose–response curve is symmetrical like a real bell. In extreme cases the descending limb may be almost vertical or almost horizontal; the decisive element to designate a dose–response curve bell-shaped is (besides the presence of an ascent) the presence of a descent regardless of its steepness.] The Recovery Model is intended to explain the occurrence and shapes of the inhibitory limbs, i.e. the descents, of bell-shaped dose–response curves by a novel and simple kinetic analysis of the operation cycle of a macromolecule.

The paper is organized as follows. First we describe the basic features of the Recovery Model and perform a mathematical analysis on the basis of a minimal version of the model. Subsequently we point out a number of implications of the Recovery Model; after that we discuss at length essential characteristics, limitations and some possible refinements and extensions of the Recovery Model as well as its relationship to previous models of HLI. Finally we briefly comment on the conceptual linkage of HLI to other non-Michaelian phenomena and the paradigmatic role the Recovery Model may play in situations in which reactions with intrinsically different time structures compete with each other.

Part of this work has been published in preliminary form [2–5].

Abbreviations used: HLI, inhibition by high ligand concentrations; L, ligand; M, M*, M**, M', (macro)molecule in the resting, active, superactive and refractory state respectively.

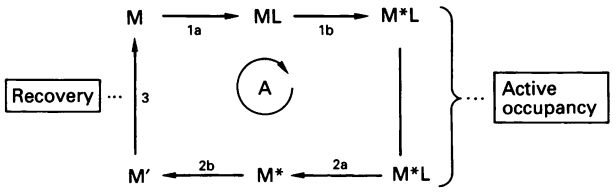

Figure 1 The basic cycle

L, ligand; M, M* and M′, resting, active and refractory state of the macromolecule; A, cycle A which is the basic operating cycle of the macromolecule. The arrows indicate the various reactions (association, dissociation, isomerization). A line without an arrowhead indicates in this and all subsequent Figures a state of the liganded macromolecule to which special attention is paid. The state of active occupancy is considered to be continuous, possible intervals of inactivity due to 'flickering' being ignored here.

THE RECOVERY MODEL

Figure 1 depicts the basic reaction cycle (subsequently called cycle A) through which the macromolecule M passes after interaction with a ligand L. In the absence of the ligand the macromolecule stays in its resting state, M; however, in the presence of the ligand, the macromolecule, as a consequence of its association with the ligand, undergoes a transition (isomerization) from state M to the active state M* and subsequent to dissociation of the ligand returns to the resting state M via a refractory state M′ (inactive and non-activatable). The circulation of the macromolecule around the closed path 1a, 1b, 2a, 2b and 3 is assumed to be strictly sequential and unidirectional and the anticlockwise reactions are ignored (for justification see the Discussion section). The most important part of cycle A is the period of active occupancy during which, in the case of an enzyme, the ligand (substrate) is chemically transformed or, in the case of a hormone or neurotransmitter receptor, a signal is produced and transduced to another component or compartment (for instance, by opening of an ion channel). A further essential characteristic of the cycle is that deactivation (M* → M) does not follow the same pathway as activation (M → M*), as deactivation includes a 'recovery' step (reaction 3) from the non-activatable state M′ to the activatable state M. In principle, all three isomeric states (M, M*, M′) are thought to be able to bind the ligand. As, however, unliganded M* and M′ are assumed to decay rapidly to M, the ligand at low concentration has no significant change of associating with M* or M′; it binds only to M and thus maintains the continual running of cycle A without the occurrence of side reactions. However, when the ligand concentration is raised to higher levels, the mean association times for the reactions M + L → ML, M* + L → M*L and M′ + L → M′L become correspondingly shorter. As the ligand concentration reaches supramaximal levels, side reactions can no longer be ignored and Figure 1 has to be extended accordingly (see Figure 2). In Figure 2(a), two branch points, one at M* leading to cycle C and one at M′ leading to cycle B, are included. For the purposes of this paper we will assume that M* is much shorter lived than the mean association time for the reaction M* + L → M*L, so that cycle C can be neglected (see Figure 2b). This situation gives rise to HLI. It should be noted, however, that in situations where the reaction M* + L → M*L becomes relevant, it could give rise to a phenomenon opposite to HLI, namely high-dose (or excess-substrate) activation (see Figure 2c). The same activation could also arise when M′ in Figure 2(b) is replaced by M**, a superactive form of the macromolecule. Activation by high ligand concentrations is less frequently encountered in the literature than HLI and is not dealt with further here.

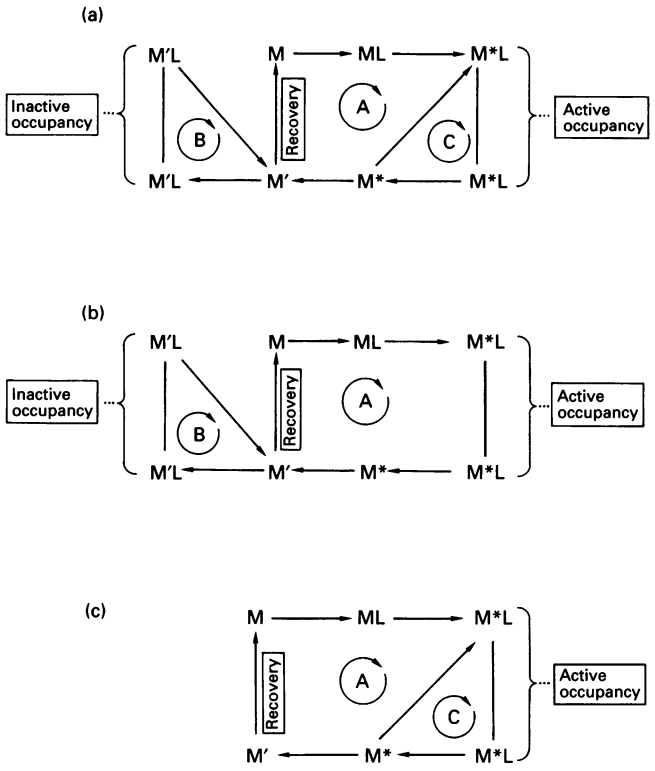

Figure 2 Extensions of the basic cycle

(a) The basic cycle A with two accessory cycles (B and C) arising at high ligand concentration. (b) The basic cycle A with the accessory cycle B giving rise to HLI. (c) The basic cycle A with the accessory cycle C giving rise to activation by high ligand concentration.

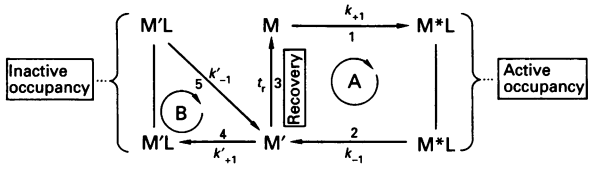

Figure 3 A minimal model for HLI

For the association reactions 1 and 4 and the dissociation reactions 2 and 5, the rate constants are indicated; for the isomerization reaction 3 (recovery), the fixed recovery time t_r is given. The quantitative treatment of the scheme is given in the Appendix.

For the sake of clarity and in order to make the mathematical analysis as tractable as possible, we analyse HLI on the basis of a minimal model which ignores the short-lived intermediates ML and M* (see Figure 3). Although the scheme of Figure 3 is clearly an oversimplification, it is capable of explaining, at least semi-quantitatively, a large body of experimental data concerning HLI (see below). The essential features of the minimal model in Figure 3 can be summarized as follows. (i) The ligand binds to M and M′ with the rates $k_{+1}L$ and $k'_{+1}L$ respectively. Dissociation takes place with the rate constants k_{-1} and k'_{-1}. (ii) The complex M*L is active; all other forms of the macromolecule are inactive. The average activity can be calculated from the proportion of time spent in the active state (M*L). (iii) The macromolecule is trapped in its inactive and non-activatable form M′ by binding to L. (iv) The crucial point at which it is decided whether the macromolecule follows cycle A or cycle B is the branch point at M′ where reactions 3 and 4 compete with each other. (v) In

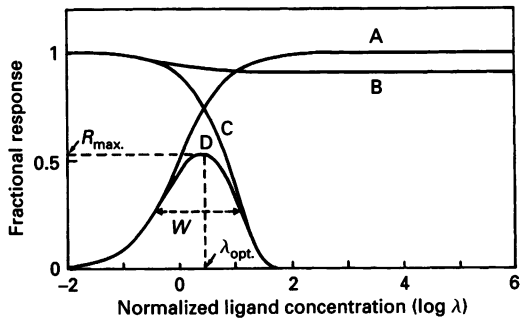

Figure 4 Constituents and characteristics of a bell-shaped dose–response curve

The abscissa represents the logarithm of the normalized ligand concentration $\lambda = L/K_d$ with $K_d = k_{-1}/k_{+1}$ and spans eight orders of magnitude. The ordinate represents the normalized response which ranges between 0 (no response) and 1 (theoretical maximum response). Curve A is a Michaelis–Menten curve and represents the activation of the macromolecule M by binding of the ligand. Curves B and C represent the inhibition of the response due to the refractory time t_r and cycle B of Figure 3 respectively. Curve D, the dose–response curve, is the product of curves A, B and C. The dose–response curve depicted here is identical with curve Ib in Figure 5. $R_{max.}$ is the maximally achievable response. The optimal ligand concentration $\lambda_{opt.}$ is the normalized ligand concentration at which $R_{max.}$ is obtained. The curve width, W, is the distance between the points of half-maximal activation and half-maximal inhibition of the dose–response curve.

kinetic terms, reaction 3 (recovery) is characterized by a fixed recovery time t_r, whereas reaction 4 (association) is characterized by the mean association rate $k_{+1}L$ which is proportional to the ligand concentration. The probability P that reaction 3 takes place instead of reaction 4 is therefore given by the probability that the reaction $M' + L \rightarrow M'L$ does not occur before time t_r. This is a waiting time process which is described by a Poisson distribution so that $P = \exp(-k'_{+1}Lt_r)$ (see the Appendix). The presence of the exponential term introduces an asymmetry into the dose–response curve.

A quantitative treatment of the Recovery Model according to Figure 3 is given in the Appendix. The resulting dose–response curve (see Figure 4 for an illustrative example) can be dissected, at least conceptually, into three component curves (see curves A, B and C in Figure 4) with the following meanings. (a) Curve A is a classical Langmuir binding isotherm which is identical with a Michaelis–Menten curve and reflects cycle A of Figure 3 without consideration of the intermediate refractory state M′ as if activation would follow the simple equation $M + L \rightleftharpoons M^*L$. (b) Curve B expresses the inhibition of the response due to the refractory time t_r. This inhibition is considerable when t_r is of the same order of magnitude as the mean life time $\tau_{occ.} = 1/k_{-1}$ of M*L; it is negligible when the ratio $T = t_r/\tau_{occ.} \ll 1$. (c) Curve C represents the inhibition of the response due to cycle B of Figure 3 and is responsible for the occurrence of HLI. As curve C contains exponential constituents (see the Appendix), it can never strictly adopt the shape of a Langmuir binding isotherm. Curve D in Figure 4 is the dose–response curve which is the product of curves A, B and C.

Variation of the kinetic parameters gives rise to a wide variety of dose–response curve shapes (see Figure 5). In each of the graphs in Figure 5, the abscissa represents the logarithm of the normalized ligand concentration $\lambda = L/K_d$ with $K_d = k_{-1}/k_{+1}$. The ordinate represents the normalized response which ranges from 0 (no response) to 1 (theoretical maximum response). The nine cases depicted in Figure 5 correspond to different combinations of $A = K_d/K'_d$ and $B = k'_{-1}/k_{-1}$. The individual curves,

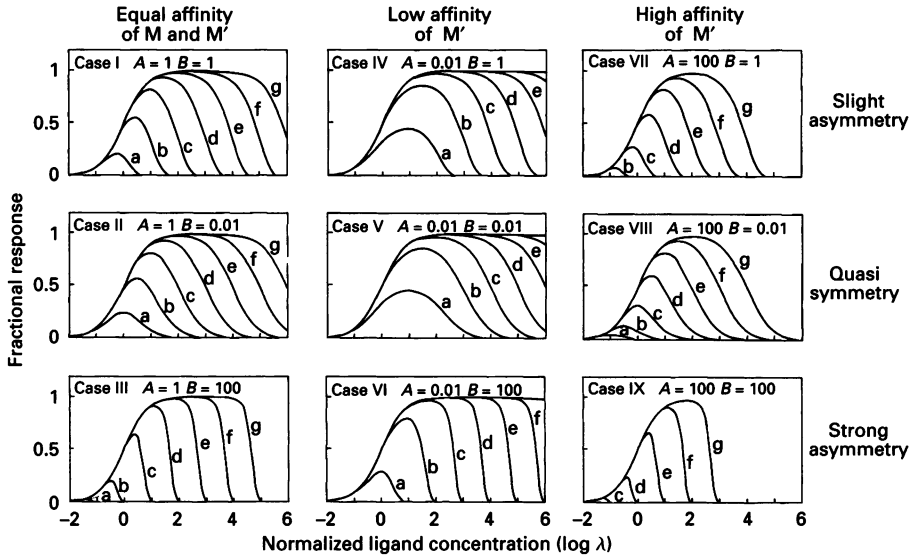

Figure 5 Representative examples of dose–response curves obtained on the basis of Figure 3

All curves were computer-drawn according to the mathematical formalism given in the Appendix. Abscissa and ordinate are identical with those in Figure 4. A equals K_d/K'_d and B equals k'_{-1}/k_{-1}. K_d and K'_d are the equilibrium dissociation constants of ML and M′L respectively; for the meaning of the dissociation rate constants k_{-1} and k'_{-1} see Figure 3. Curves a, b, c, d, e, f and g are those obtained for $T = 1$, 10^{-1}, 10^{-2}, 10^{-3}, 10^{-4}, 10^{-5} and 10^{-6} respectively, with $T = t_r k_{-1} = t_r/\tau_{occ.}$. The nine sets of curves correspond to the following Cases I–IX: Case I, $K'_d = K_d$, $k'_{+1} = k_{+1}$, $k'_{-1} = k_{-1}$ (equal affinity of M′ and M); at all values of T the descent is somewhat steeper than the ascent (slight asymmetry). Case II, $K'_d = K_d$, $k'_{+1} = 0.01 \times k_{+1}$, $k'_{-1} = 0.01 \times k_{-1}$ (equal affinity of M′ and M); although the dose–response curves look quite symmetrical, numerical evaluation reveals that the descending limb is always somewhat steeper than the ascending limb (quasisymmetry). Case III, $K'_d = K_d$, $k'_{+1} = 100 \times k_{+1}$, $k'_{-1} = 100 \times k_{-1}$ (equal affinity of M′ and M); at all values of T (except $T = 1$) the descent is much steeper than the ascent (strong assymetry). Case IV, $K'_d = 100 \times K_d$, $k'_{+1} = 0.01 \times k_{+1}$, $k'_{-1} = k_{-1}$ (low affinity of M′). Case V, $K'_d = 100 \times K_d$, $k'_{+1} = 0.0001 \times k_{+1}$, $k'_{-1} = 0.01 \times k_{-1}$ (low affinity of M′). Case VI, $K'_d = 100 \times K_d$, $k'_{+1} = k_{+1}$, $k'_{-1} = 100 \times k_{-1}$ (low affinity of M′). Case VII, $K'_d = 0.01 \times K_d$, $k'_{+1} = 100 \times k_{+1}$, $k'_{-1} = k_{-1}$ (high affinity of M′). Case VIII, $K'_d = 0.01 \times K_d$, $k'_{+1} = k_{+1}$, $k'_{-1} = 0.01 \times k_{-1}$ (high affinity of M′). Case IX, $K'_d = 0.01 \times K_d$, $k'_{+1} = 10000 \times k_{+1}$, $k'_{-1} = 100 \times k_{-1}$ (high affinity of M′); Case IX represents an extreme situation. As far as a significant response is obtained at all, the maximal response $R_{max.}$ stays reduced even at T values as low as 10^{-6}.

Table 1 Summary of characteristics of the dose–response curves in Figure 5

For the meaning of $\lambda_{opt.}$, W, $R_{max.}$, T, K'_d, K_d, k'_{-1} and k_{-1} see Figures 3–5 or the text. ↑ means increase and ↓ means decrease.

$\lambda_{opt.}$, W and $R_{max.}$	at variable T	:	↑	if T ↓
	at variable K'_d/K_d	:	↑	if K'_d/K_d ↑
	at constant T and constant K'_d/K_d	:	↑	if asymmetry ↓

Asymmetry	: ↑ if k'_{-1}/k_{-1} ↑	(regardless of whether $K'_d >$, $=$ or $< K_d$)	
	↓ if $R_{max.}$ ↓	(significant only at relatively low $R_{max.}$)	
	Strong asymmetry*	if $k'_{-1} \gg k_{-1}$	
	Slight asymmetry	if $k'_{-1} \approx k_{-1}$	
	Quasisymmetry	if $k'_{-1} \ll k_{-1}$	

* Valid only if $R_{max.}$ is not too low.

labelled a, b, c, d, e, f and g, result from varying $T = t_r/\tau_{occ.}$ from 1 to 10^{-6}. On comparison of all curves in Figure 5, the essential characteristics of the dose–response curves obtained on the basis of Figure 3 can be summarized as follows (see also Table 1). (1) The optimal ligand concentration, $\lambda_{opt.}$, the maximal response, $R_{max.}$, and the curve width, W, increase when T decreases and/or K'_d/K_d increases. When T and K'_d/K_d are kept constant, $\lambda_{opt.}$, $R_{max.}$ and W increase when the asymmetrical character of the dose–response curve decreases (compare e.g. curve IIIa with curves Ia and IIa or curve VIa with curves IVa and Va). (2) The intrinsic asymmetry of the dose–response curve is marked as the ratio k'_{-1}/k_{-1} is increased or, in other words, the mean lifetime of M′L is decreased relative to that of M*L. Strong asymmetry can be obtained when $K'_d = K_d$ (Case III), $K'_d > K_d$ (Case VI) or $K'_d < K_d$ (Case IX). The same independence of the ratio K'_d/K_d also holds for slight asymmetry (compare Cases I, IV and VII) and quasisymmetry (compare Cases II, V and VIII). Thus the decisive determinant for strong, slight or virtually absent asymmetry is k'_{-1}/k_{-1} and not K'_d/K_d or k'_{+1}/k_{+1}.

In the model discussed above, the complex M′L is assumed to be completely inactive. As a result, HLI reduces the response asymptotically to zero if the ligand concentration is raised to a sufficiently high level and, as will be shown below (see Table 2), there exists a minimal steepness of the descending limb of the dose–response curve with an apparent Hill coefficient of 1. On the other hand, if M′L retains some partial activity, the steepness of the descending limb is decreased and can adopt 'subminimal' values and HLI is partial, i.e. inhibition due to cycle B can never depress the response down to zero level. Similarly, the shapes of the curves can be modified by inclusion of additional side reactions or internal loops. However, it is not our purpose here to present an exhaustive collection of more complicated models but, rather, to demonstrate that a simple model which incorporates an obligatory recovery step in its operation cycle can give rise to bell-shaped dose–response curves that contain many of the characteristics that are observed experimentally.

IMPLICATIONS OF THE RECOVERY MODEL

Partial agonism

In pharmacology it is well known that many (primarily synthetic) ligands of receptors can never elicit a full response and they are therefore classified as 'partial agonists'. An analogous situation is encountered in enzymology: for a given enzyme there are 'poor' substrates which are never chemically transformed at the same maximal velocity as 'good' substrates. In the following we treat both phenomena under the pharmacological term 'partial agonism'.

In principle, a change in any of the reaction steps constituting an operation cycle may lead to partial agonism. Referring to the operation cycle of Figure 1, one obvious reason for partial agonism could be that reaction 1b is relatively too slow so that, if L is not sticky, it dissociates from M to a significant extent before the latter has isomerized to M* or, if L is sticky, the macromolecule spends too much time fruitlessly in state ML. Presumably the partial agonism of many, if not most, partial agonists goes back to a situation where the overall reaction $M + L \rightarrow M^*L$ is significantly slower than in the case of a full agonist, and we call it partial agonism type 1.

The Recovery Model suggests two further explanations of partial agonism. The ratio $T = t_r/\tau_{occ.}$ may be so large that it limits the maximal response, $R_{max.}$ (see Figure 5 and curve B in Figure 4: at $T = 1$, $R_{max.}$ is limited to 50%, and at $T = 0.1$, it is limited to 90% of the theoretical maximum) (partial agonism type 2). An increase in T can be achieved by a shortened occupancy time $\tau_{occ.}$ and/or a prolonged recovery time t_r. A certain agonist may decrease $\tau_{occ.}$ but this decrease alone may not suffice to give rise to partial agonism type 2: only when T is raised to values of, say, 0.05 or more, will $R_{max.}$ be significantly reduced. Prolongation of the recovery time, t_r, by a partial agonist is perhaps a more remote possibility, but it might be envisaged that an imperfect ligand causes a greater 'deformation' of the macromolecule or departs more slowly from the active site than a perfect ligand; consequently the recovery of the macromolecule may take longer.

When partial agonism is observed at values of $T \leqslant 10^{-2}$, partial agonism type 2 cannot be considered. Figure 5 shows several examples: at $T = 10^{-2}$ (see curves Ic, IIc, IIIc, VIIc, VIIIc and IXc) and even at $T = 10^{-4}$ (see curves VIIe, VIIIe and IXe) a marked partial agonism can occur. This type of partial agonism (partial agonism type 3) is easily explained by and necessarily linked with HLI, provided that the curve width, W, does not become too large (in Figure 5, W should not exceed about two to three orders of magnitude). Thus, whereas partial agonism type 1 or 2 is not necessarily linked with HLI, type 3 is always accompanied by HLI. In practice, however, it may not always be possible to use this criterion of distinction because, for instance, a limited solubility of the ligand may prevent detection of HLI.

Pulse generation and desensitization

The Recovery Model predicts that there is no HLI as long as the ligand, albeit added at supramaximal concentration, occupies the macromolecule for the first time; only after the first active occupancy period can HLI appear as a result of the formation of M′L. In other words, an initial pulse or spike of activity which is elicited during the first occupancy period is followed by a period of inactivity which lasts as long as the ligand concentration is maintained at the supramaximal level. We call the former event 'pulse generation' and the latter 'HLI desensitization'. We shall first discuss HLI desensitization.

In contrast with the so-called acute (short-term, rapid) and chronic (long-term, slow) types of desensitization (for a review see, e.g., ref. [6]) which may occur at very low ligand concentrations (for β-adrenergic systems see, e.g., refs. [7,8]), HLI desensitization occurs only at supramaximal concentrations. Furthermore, HLI desensitization can be 'ultrarapid', as it can set in immediately after elapse of the mean lifetime of the active macromolecule–ligand complex (M*L in Figure 3) which may be as short as a few milliseconds. HLI desensitization may also be ultrarapidly reversible, as the speed of reversal is only limited by

the time needed to lower the ligand concentration from a supramaximal level to the maximal level or by the mean length of the last occupancy period of M′ which may be as short as a fraction of a millisecond. The other types of desensitization mentioned do not possess the capability for such fast kinetics of appearance and disappearance; for instance, in β-adrenergic systems [6], acute (rapid) desensitization is not detectable before the elapse of seconds or a few minutes and chronic (slow) desensitization needs minutes, sometimes several hours, to become established; similar times are usually required for the reversal. The relationships and possible interdependencies between HLI, rapid and slow desensitization are poorly understood. A system that is in a state of ultrarapid HLI desensitization might be prevented from developing a state of rapid or slow desensitization as long as the state of HLI desensitization is maintained. Such an exclusion phenomenon might explain the finding [9] that the (partial) β-adrenergic agonist ICI 89963 at high concentration autoinhibits its ability to chronically desensitize C6 rat glioma cells.

The obligatory sequence of events, first the elicitation of an activity spike or pulse when the ligand concentration is suddenly increased and then an immediate decrease in activity due to the onset of HLI desensitization, endows the activity spike with a strong signal character. Phenomenologically, the situation bears some resemblance to a neurotransmitter-elicited postsynaptic current or action potential which is followed by a period of refractoriness, and we suggest that HLI desensitization might be an essential factor for a full understanding of how the shapes of postsynpatic potentials are determined. A detailed discussion of autoinhibition phenomena in neurotransmitter receptor systems, e.g. the neuromuscular junction, is, however, beyond the scope of this paper.

Memory effects

The Recovery Model implies that the macromolecule 'remembers' its interaction with the ligand for a certain length of time which is identical with t_r (see Figure 3); so the subscript r stands for recovery, refractoriness and recall. This memory is short-lived and not carried over from one cycle A to another; rather it has to be extinguished in order to complete cycle A and to allow the restart of a new cycle A. If, however, the macromolecule encounters the ligand again before it has lost the memory of its past interaction with the ligand, the memory is kept alive and the macromolecule behaves differently: it will not re-enter a new cycle A after reassociation with the ligand. The memory of the macromolecule is nonetheless a short-term one, as even after many successive reassociations, i.e. after many circulations through cycle B of Figure 3, the macromolecule will not remember the last ligand interaction longer than after only one association.

These characteristics distinguish the Recovery Model from the concept of a 'hysteretic' enzyme with a slow conformational transition which seems to require multiple catalytic cycle turnovers before the enzyme reaches a new conformational state [10–14]. Ricard et al. [12,15] called this transition a 'mnemonical transition' which is, according to Neet and Ainslee [14], thought to occur outside the normal catalytic reaction path and never during the period of the first catalytic cycle. The original formulation of the mnemonical enzyme concept by Ricard et al. [15] did not contain the restrictive assumption that the mnemonical transition has to be slow; moreover, the original mnemonical model (see Figure 1 in [15]) has much in common with the minimal Recovery Model of Figure 3. However, the treatment in [15], contrary to a conceptually similar treatment by Witzel and co-workers [16–18], negated the possibility of substrate inhibition for a mnemonical enzyme.

Long-term memory effects as described for hysteretic enzymes are not considered in the Recovery Model described in this paper; it is, however, conceivable that a macromolecule can memorize the interaction with the same ligand both in short-term and long-term fashion. How a long-term memory can be established by a cumulative effect of repeated on/off cycles of the ligand or by a long-lasting after-effect of only one critical encounter of ligand and macromolecule is an unsolved problem.

Ultrasensitivity

The mathematical analysis of the Recovery Model according to Figure 3 reveals that the inhibitory limb of the dose–response curve is very steep if $k'_{-1} \gg k_{-1}$ and $R_{max.}$ is not too small (see curves IIIc–g, VIb–f and IXe–g of Figure 5 where this situation is exemplified for $k'_{-1} = 100 \times k_{-1}$). Thus in a certain range of ligand concentration the system can respond extraordinarily sensitively to a small increase or decrease of the ligand concentration. This type of 'ultrasensitivity' [19], termed by us 'HLI ultrasensitivity', represents a new type of 'branch-point ultrasensitivity' [20,21], as HLI ultrasensitivity is a consequence of a branch point where two reactions (reactions 3 and 4 in Figure 3) compete with each other. It may be noted that HLI ultrasensitivity can be obtained even if, as assumed in the minimal model of Figure 3, both macromolecular species, M and M′, bind the ligand according to a simple Langmuir isotherm and even if (see Case III in Figure 5) M and M′ have the same affinity for the ligand. In the case of $k'_{-1} = 100 \times k_{-1}$ and $R_{max.} \geqslant 0.9$ (see curves IIId–g, VIc–f and IXf,g in Figure 5) the HLI ultrasensitivity of a Langmuir-type monoligandable macromolecule is equivalent to the ultrasensitivity of an allosteric protein with a Hill coefficient (h) of about 5. The dependence of the apparent Hill coefficient of the descent of the dose–response curve on the ratio $B = k'_{-1}/k_{-1}$ is shown in Table 2 for a wide range of B values (from 10^{-6} to 10^{6}). Whereas at low values of B the apparent Hill coefficients approach 1, an increase in B to very high values does not cause h to approach an upper finite value. In other words, the minimal model according to Figure 3 yields for the descent of the dose–response curve a minimal steepness of

Table 2 Apparent Hill coefficients of the descent of the dose–response curves in dependence on $B = k'_{-1}/k_{-1}$

The apparent Hill coefficients were calculated as shown in the Appendix. Inhibition curves with $T = 10^{-6}$ and $A = 1$ were used for calculation. Very similar apparent Hill coefficients were obtained for $A = 0.01$ and $A = 100$ (not shown).

B	Apparent Hill coefficient
10^{-6}	1.00
10^{-5}	1.00
10^{-4}	1.00
10^{-3}	1.00
10^{-2}	1.01
10^{-1}	1.05
1	1.47
10	2.86
10^{2}	4.85
10^{3}	7.06
10^{4}	9.32
10^{5}	11.62
10^{6}	14.02

$h = 1$ whereas the maximal steepness of the descent appears to correspond to the vertical ($h = \infty$). The latter phenomenon represents an extremely sharp switch on/switch off mechanism at a certain ligand concentration.

DISCUSSION

The importance of non-occupancy

In the interaction of a ligand and a macromolecule, periods of occupancy alternate with periods of non-occupancy. Attention is usually paid only to the state of occupancy because it is during this phase that the response occurs or is at least initiated. The period of non-occupancy has been widely regarded as unimportant but unavoidable as the time interval between dissociation and reassociation is always of finite length even at the highest ligand concentrations physically possible. When genuine HLI (and not a pseudo form caused by e.g. impurities or inadequacies of the analytical method) was observed under such conditions, it was usually interpreted in the light of occupancy and attributed to an increased multiplicity of occupancy (Haldane mechanism) or to an otherwise abortive occupancy. (For a brief review of previously proposed mechanisms for explanation of substrate inhibition, see ref. [5].) To our knowledge, HLI has never before been attributed explicitly to a period of non-occupancy that is too short. We propose that non-occupancy of one or more ligand-binding sites is usually an essential constituent of the working cycle of a macromolecule (postulate of obligatory non-occupancy) in the same way as, at a much higher level of biological organization, sleep is an essential part of the daily working cycle of man. The Recovery Model presented in this paper rests on this simple idea. The occurrence of HLI in the minimal Recovery Model of Figure 3 depends on whether the non-occupancy period of M′ is shorter or longer than the recovery time t_r. Experimental tests of the applicability of the Recovery Model for explanation of HLI should be aimed at detection of M′ by an appropriate intrinsic or extrinsic probe and the kinetic characterization of M′ in dependence of the ligand concentration.

The fixed recovery time, t_r

In contrast with occupancy and non-occupancy times, which are treated as statistical mean values because of the stochastic character of dissociation and association reactions, the recovery process M′ → M (reaction 3 in Figure 3) is assumed to be not subject to the same statistical variation but rather to be fixed, i.e. with a negligibly small variance. This has the consequence that the resulting bell-shaped dose–response curves become more or less asymmetrical and thus may more truly reflect experimental curves which often deviate appreciably from symmetry. Were the recovery time in the minimal model of Figure 3 not fixed but of a Poissonian (exponential) character like a conventional relaxation time, the resulting dose–response curves could never adopt an asymmetric shape (not shown) and the Recovery Model would lose much of its versatility and explicatory power. The fixed duration of the recovery process is a feature that distinguishes the Recovery Model from previous conceptually related models.

Can the assumption of a fixed recovery time be justified? It seems that the justification has to arise from the nature of the isomerization process underlying recovery. If recovery is a multistep (conformational or other kind of) process involving a large number of sequential individual steps, then the time needed for the overall reaction M′ → M does not have a Poisson distribution but is restricted to a narrow range of time periods; in other words, the recovery time t_r is quasideterministically fixed. The phenomenon that the transition time from one state to another state can be virtually fixed if the transition occurs via a sufficiently large number of intermediate states has been reported previously in various contexts [22–24].

The non-identity of the activation pathway M → M* and the deactivation pathway M* → M

This feature of the model, which is caused by the obligatory passage through the refractory state M′ during the deactivation pathway M* → M, is in accordance with the frequently encountered phenomenon in biology that different paths are followed for the forward and reverse reactions (e.g. a non-congruity of anabolic and catabolic pathways in intermediary metabolism, divergent routes for biosynthesis and degradation of macromolecules and for assembly and disassembly of supramolecular structures such as viruses, microtubuli etc.). More specifically, the non-identity of the reactions M → M* and M* → M might be, at least in some cases, comparable with unfolding (denaturation) and refolding (renaturation) of macromolecules, which often follow, at least partly, different pathways.

The unidirectionality of cycle A

All reactions constituting cycle A (see Figures 1–3) are shown in one (clockwise) direction only, as if the corresponding reverse (anticlockwise) reactions did not exist. Is this simplification justifiable? To answer this question we must take into account the following. (i) We are considering only a steady state and not equilibrium, in agreement with the relatively rare occurrence of true thermodynamic equilibrium in biological systems. A working enzyme, for instance, is in a steady state or a transient state rather than in equilibrium and can therefore be likened to a 'turning wheel' [25,26]. (ii) A steady state implies that the system is free of the constraint of detailed balance [25,27–30], i.e. the product of the forward rates is not equal to the product of the backward rates. When the reactions are linked to a closed cycle and the same macromolecule is involved in all reactions, a unidirectional circulation of the macromolecule around the cycle results, either clockwise or anticlockwise depending on whether the product of the forward rates is larger or smaller than the product of the backward rates. In the special case where one of the two products is much smaller than the other, one can neglect the reactions in that direction. Such a situation applies to cycle A of the Recovery Model, as we assume that at least one of the isomerization reactions M → M*, M* → M′ and M′ → M is quasi-irreversible so that the product of all backward rates of cycle A becomes much smaller than the product of all forward rates. Thus the mathematical analysis of cycle A can be performed without consideration of the backward reactions.

Possible modifications and extensions of the minimal Recovery Model

As stated previously, the Recovery Model in its simplest form (see Figure 3) is regarded as a minimal model; as such it is sufficient to demonstrate the key point of our explanation of HLI, namely non-occupancy times of M′ that are too short at supramaximal ligand concentrations. This simple assumption yields a large variety of dose–response curves which display differences in the shape and position of the descending limb (see Figure 5). On the other hand, the Recovery Model according to Figure 3 is certainly an oversimplification and cannot be expected to explain all of the bell-shaped dose–response curves that have been obtained in pharmacology and enzymology for a number of

possible reasons. (i) For many binding/activation processes a Hill coefficient (h) different from 1 is observed, whereas we assumed for simplicity that both M and M′ bind the ligand in a Michaelis–Menten or Langmuir fashion, i.e. with $h = 1$. Clearly, in the case where M is activated only after binding of two or more ligand molecules to two or more interacting sites would the ascents of the resulting dose–response curves adopt different shapes. Similarly, it can be envisaged that the branching to an inactive pathway in some cases requires double or multiple occupancy of M′. It is obvious that binding processes with $h \neq 1$ would cause the resulting dose–response curves to change correspondingly. (ii) The recovery time, t_r, may not be absolutely fixed but subject to a significant statistical variation; this can modify the degree of asymmetry of the dose–response curve. In the extreme case in which the recovery reaction of step 3 (see Figure 3) is a simple Poisson process, as is assumed for the association reaction of step 4, the intrinsic asymmetry of the dose–response curves vanishes (not shown). (iii) The recovery process may not start exactly at the instant of dissociation of the M*L complex, as assumed in the scheme of Figure 3. Rather, it may start either somewhat later, as indicated in Figures 1 and 2, or somewhat earlier, i.e. still during occupancy of the macromolecule by the ligand. In the latter case, the importance of non-occupancy would be more or less attenuated and M′ would be less vulnerable to untimely arrival of ligands. In the extreme case in which the recovery process goes to completion during occupancy, the macromolecule would not be inhibited at all by high ligand concentrations (HLI resistance due to elimination of vulnerable periods of non-occupancy). (iv) Binding of L to M′ may disturb the recovery process in different ways and to different degrees. In the most drastic case (as implicitly assumed in the scheme of Figure 3), L fully reverses the recovery process regardless of how far the latter has advanced at the instant of association of L to M′, so that the recovery process has to restart from the very beginning after each association with L. Milder forms of disturbance are partial reversion, standstill or only a decelerated advancement of the recovery process. In the last case, only partial HLI can be obtained, i.e. the inhibition stays partial even at an infinitely high concentration of L. It remains to be analysed in detail how the various ways of disturbing the recovery process may alter the shape and/or position of the descending limbs of the dose–response curves. (v) The association reaction, $M' + L \rightarrow M'L$, may not be a simple Poisson process. For instance, if the arriving ligand molecules first have to pass a 'waiting room' (an accessory binding site at the same or a neighbouring macromolecule), at high ligand concentrations the interarrival times at the active site may be quite different with respect to size and statistical variation from the time intervals with which the ligands arrive from the bulk at the accessory site. Waiting rooms may convert the random pattern of arrival events to a more regular one and create a 'time buffer' zone between vacation and reoccupation of the active site. By such a waiting room device, the macromolecule may be enabled to recover undisturbed even at very high ligand concentrations (HLI resistance due to time buffering by waiting rooms). (vi) The backward (anticlockwise) reactions in cycle A of Figure 3 (or more complex reaction schemes) are not negligible if the product of all backward rates is larger than, say, 5% of the product of all forward rates. In this case the rotation of the 'turning wheel' [25], i.e. the speed of cycle A in the clockwise direction, is slowed down and, correspondingly, the maximal response is decreased. (vii) An additional activation cycle C (see Figure 2a) which counteracts cycle B may be present and might under certain conditions give rise to rather complex (undulating or 'bumpy') dose–response curves.

In summary, the Recovery Model according to Figure 3 is clearly a minimal model which needs refinements and extensions (some of which are listed above) to conform with the complexities of a real system and to reproduce quantitatively the whole spectrum of actually observed dose–response curves. Nevertheless, the concept that HLI can be explained by trapping of a refractory state M′ as a result of a too short non-occupancy time of M′ is applicable to any Recovery Model regardless of whether it is formulated as a minimal model or as a highly sophisticated model.

What distinguishes the Recovery Model from previously proposed models for explaining HLI?

Models that do not require an increased number of simultaneously bound ligand molecules or a changed order of ligand addition or a ligand-dependent change of the aggregation state of the macromolecule have been previously proposed, although not very often; like the Recovery Model, they only require that a high ligand concentration favours an inactive or less active isomer of the macromolecule. Such pure isomerization or, briefly [31,32], 'Iso' mechanisms (especially conformational mechanisms) of HLI have been considered in particular for monomeric one-substrate enzymes [16–18,33–37], thus avoiding the postulation of one or more additional ('regulatory') substrate-binding sites or binding of a new substrate molecule before all products have been released.

Although the Recovery Model presented in this paper shares with previous Iso models the basic assumption that a high ligand concentration favours a 'wrong' (i.e. inactive or less active) isomeric form of the macromolecule, it differs fundamentally in the following points from the previous (Iso and other) models of HLI. (i) The Recovery Model contains in its various reaction schemes (see Figures 1–3) a step, the recovery reaction $M' \rightarrow M$, that cannot be described by a conventional rate constant k or its reciprocal, a relaxation time τ, as the time evolution of this reaction does not obey an exponential function like that of a conventional relaxation process but follows, as an approximation, a step function with a fixed first passage time t_r (for justification see above). We therefore used the Latin symbol t instead of the recommended [38] and widely used Greek symbol τ to designate the time required for the recovery reaction to occur. (ii) The Recovery Model contains a branch point (see Figures 2a, 2b and 3) where two reactions (reactions 3 and 4 in Figure 3) with intrinsically different time structures compete with each other: an association reaction ($M' + L \rightarrow M'L$) of simple Poissonian character and an isomerization reaction ($M' \rightarrow M$) of fixed duration. To treat such a situation quantitatively, we introduced a queue-theoretical element in our model: we regarded the binding of the ligand L to the macromolecule as a waiting time process where L has to wait till the fixed recovery time t_r has elapsed in order to enter a new active cycle A; otherwise L enters the inactive cycle B. Our stochastic queue-theoretical treatment of the reaction scheme of Figure 3 yielded results that are not obtainable by applying conventional steady-state kinetics with conventional rate constants to a reaction scheme as simple as that of Figure 3. The latter approach, which would describe the recovery step in Figure 3 by a conventional rate constant k, would yield only strictly symmetrical dose–response curves and could not generate descents with a Hill coefficient larger than 1 (not shown).

Outlook and final comments

Situations in which, analogously to reactions 3 and 4 in Figure

3, association and isomerization reactions compete and interact with each other may not be uncommon; they may occur at any phase of the operation cycle of a macromolecule and give rise to inhibitory or activating 'epicycles' analogous to cycles B and C in Figure 2. The macroscopic consequence of such competition situations is usually a deviation of the dose–response curve from a Michaelis–Menten shape. This deviation is upwards in the case of activating epicycles, downwards in the case of inhibitory epicycles and may occur not only at a high range but at any range of the ligand concentration. Furthermore, when one considers the great influence a different time structure of two competing reactions may exert on the extent of the deviation mentioned, exemplified by the interplay of reactions 3 and 4 in Figure 3, a great shape variability of the ascending limbs of dose–response curves is also to be expected. Thus any kind of non-Michaelian behaviour may be caused by a purely temporal mechanism, namely positive or negative timing effects of (usually randomly) arriving ligand molecules during timing-sensitive phases of the operation cycle of the macromolecule. Contrary to the conventional allosteric models [39,40], no multiple ligand-binding sites are required: allochronic [41] binding (i.e. binding at different times during the operation cycle) at a single site can be sufficient to elicit a non-Michaelian response; but even if spatial summation of ligand binding to multiple sites occurs, the proper temporal relationships between the binding events at locally distant but interacting sites may still be crucial [4], analogous to well-known phenomena in neurophysiology [42]. Allochrony provides a new conceptual basis for understanding non-Michaelian behaviour and a conceptual linkage between phenomena that have usually been regarded as unrelated (e.g. HLI and sigmoidicity or other kinds of 'non-hyperbolicity' in non-logarithmic plots of response versus ligand concentration).

The Recovery Model presented in this paper should not be qualified merely as another variation in the collection of existing models for explanation of HLI. Rather, our model possesses features that distinguish it fundamentally from previous models of HLI (see above) and, in addition, appear relevant in a much wider context; we would like to mention the following points. (i) The mathematical analysis of the minimal Recovery Model (Figure 3) is the first quantitative application of the concept of allochrony; the latter is based on the assumption that (a) a working macromolecule traverses during its operation cycle several temporal phases and various states of excitability and refractoriness [4] and (b) ligand molecules arriving at different times (i.e. allochronically) during the operation cycle either activate or inhibit the macromolecule, depending on the phase during which the macromolecule is hit and occupied by the ligand molecules. (ii) We have shown that even an extremely simplified kinetic scheme (see Figure 3) can yield a remarkable shape diversity of the dose–response curves (see Figure 5). We achieved this by breaking with the kineticists' habit of routinely applying a conventional rate constant k to every reaction step, and we consider it as a major merit of the Recovery Model that it draws attention to the generally relevant fact that the uncritical application of conventional rate constants may lead to false results. For situations in which two reactions with intrinsically different time structures (like reactions 3 and 4 in Figure 3) compete with each other, the Recovery Model may serve as a paradigm. (iii) Finally, the Recovery Model is a clear-cut example of the usefulness of a stochastic approach in enzyme and receptor kinetics. Stochastic treatments are not popular among kineticists, but we think there exist several situations for which only a stochastic approach yields the correct result; the same opinion has been expressed in a different context by other authors [43].

The mathematical assistance of Dr. W. B. Adams is gratefully acknowledged.

REFERENCES

1 Langenbeck, W. (1935) Die organischen Katalysatoren and ihre Beziehungen zu den Fermenten, p. 70, Verlag von Julius Springer, Berlin
2 Kühl, P. W. and Adams, W. B. (1985) in Pharmacology of Adrenoceptors (Szabadi, E., Bradshaw, C. M. and Nahorski, S. R., eds.), pp. 305–306, Macmillan Press, Basingstoke and London
3 Kühl, P. W. (1988) Biol. Chem. Hoppe-Seyler **369**, 1204
4 Kühl, P. W. (1990) Eur. J. Pharmacol. **183**, 1547–1548
5 Kühl, P. W. (1992) in Biocatalysis in Non-Conventional Media (Tramper, J., Vermuë, M. H., Beeftink, H. H. and von Stockar, U., eds.), pp. 245–252, Elsevier, Amsterdam
6 Perkins, J. P., Harden, T. K. and Harper, J. F. (1982) in Handbook of Experimental Pharmacology (Nathanson, J. A. and Kebabian, J. W., eds.), vol. 58, pp. 185–224, Springer-Verlag, Berlin
7 Franklin, T. J., Morris, W. P. and Twose, P. A. (1975) Mol. Pharmacol. **11**, 485–491
8 Krall, J. F., Connelly, M. and Tuck, M. L. (1980) J. Pharmacol. Exp. Ther. **214**, 554–560
9 Franklin, T. J. and Twose, P. A. (1979) J. Cyclic Nucl. Res. **5**, 19–30
10 Frieden, C. (1970) J. Biol. Chem. **245**, 5788–5799
11 Ainslee, G. R., Jr., Shill, J. P. and Neet, K. E. (1972) J. Biol. Chem. **247**, 7088–7096
12 Ricard, J., Buc, J. and Meunier, J.-C. (1977) Eur. J. Biochem. **80**, 581–592
13 Frieden, C. (1979) Annu. Rev. Biochem. **48**, 471–489
14 Neet, K. E. and Ainslee, G. R., Jr. (1980) Methods Enzymol. **64**, 192–226
15 Ricard, J., Meunier, J.-C. and Buc, J. (1974) Eur. J. Biochem. **49**, 195–208
16 Witzel, H., Rübsamen, H., Khandker, R., Kaiser, P. and Müller, R. (1973) in Ribosomes and RNA Metabolism (Zelinka, J. and Balan, J., eds.), pp. 431–446, Publishing House of the Slovak Academy of Sciences, Bratislava
17 Rübsamen, H., Khandker, R. and Witzel, H. (1974) Hoppe-Seyler's Z. Physiol. Chem. **355**, 687–708
18 Kaiser, P. M. (1980) J. Mol. Cat. **8**, 431–442
19 Koshland, D. E., Jr., Goldbeter, A. and Stock, J. B. (1982) Science **217**, 220–225
20 LaPorte, D. C., Walsh, K. and Koshland, D. E., Jr. (1984) J. Biol. Chem. **259**, 14068–14075
21 Koshland, D. E., Jr. (1987) Trends Biochem. Sci. **12**, 225–229
22 Deshcherevskii, V. I., Zhabotinskii, A. M., Sel'kov, Y. Y., Sidorenko, N. P. and Shnol', S. E. (1970) Biophysics **15**, 235–245 (Russian original: Biofizika **15**, 225–234)
23 Morozov, V. N. (1972) Biophysics **17**, 974–977 (Russian original: Biofizika **17**, 926–929)
24 Easterby, J. S. (1984) Biochem. J. **219**, 843–847
25 Wyman, J. (1975) Proc. Natl. Acad. Sci. U.S.A. **72**, 3983–3987
26 Careri, G. and Wyman, J. (1984) Proc. Natl. Acad. Sci. U.S.A. **81**, 4386–4388
27 Klein, M. J. (1955) Phys. Rev. **97**, 1446–1447
28 Bak, T. A. (1963) Contributions to the Theory of Chemical Kinetics. A Study of the Connection between Thermodynamics and Chemical Rate Processes, p. 29, W. A. Benjamin, New York, and Munksgaard, Copenhagen
29 Phillipson, P. E. and Wyman, J. (1980) Biopolymers **19**, 857–883
30 Agu, M. and Asami, S. (1985) J. Appl. Phys. **57**, 4839–4842
31 Cleland, W. W. (1963) Biochim. Biophys. Acta **67**, 104–137
32 Fromm, H. J. (1979) Methods Enzymol. **63**, 42–53
33 Botts, J. (1958) Trans. Faraday Soc. **54**, 593–604
34 Keleti, T. (1968) Acta Biochim. Biophys. Acad. Sci. Hung. **3**, 247–258
35 Kaiser, P. M. (1972) Doctoral dissertation, University of Marburg
36 Müller, R. (1975) Doctoral dissertation, University of Münster
37 Wells, B. D., Stewart, T. A. and Fisher, J. R. (1976) J. Theor. Biol. **60**, 209–221
38 Nomenclature Committee of the International Union of Biochemistry (1982) Eur. J. Biochem. **128**, 281–291
39 Monod, J., Wyman, J. and Changeux, J.-P. (1965) J. Mol. Biol. **12**, 88–118
40 Koshland, D. E., Jr., Némethy, G. and Filmer, D. (1966) Biochemistry **5**, 365–385
41 Kühl, P. W. (1987) Biol. Chem. Hoppe-Seyler **368**, 1069
42 Harmon, L. D. (1962) in Self-Organizing Systems 1962 (Yovits, M. C., Jacobi, G. T. and Goldstein, G. D., eds.), pp. 177–202, Spartan Books, Washington
43 Arányi, P. and Tóth, J. (1977) Acta Biochim. Biophys. Acad. Sci. Hung. **12**, 375–388

APPENDIX

We assume, as discussed in the main paper, that the macromolecule follows a unidirectional path around cycle A in Figure 3 of the main paper. We assume further that the macromolecule remains refractory for a fixed period of time, denoted as t_r.

For any reaction step that proceeds with a rate constant k, the average time required for that reaction to occur is $1/k$. This follows from an integration of t multiplied by $k\exp(-kt)$ the probability density function for a Poisson process:

$$\int_0^\infty tk\exp(-kt)\,dt = -\left(t+\frac{1}{k}\right)\exp(-kt) = \frac{1}{k} \qquad \text{(A1)}$$

Thus, the average time spent for association of a ligand molecule at concentration L is $1/k_{+1}L$ and the average time for its dissociation is $1/k_{-1}$.

The average length of time of the active cycle (cycle A) is

$$t(\text{active cycle}) = t_r + \frac{1}{k_{+1}L} + \frac{1}{k_{-1}} \qquad \text{(A2)}$$

and the average time spent in the active state (M*L) is

$$t(\text{active state}) = \frac{1}{k_{-1}} \qquad \text{(A3)}$$

The probability that the active cycle will be entered from the branch point is simply the probability that the ligand molecule does not bind to the macromolecule in the refractory state M′ before time t_r. As the association rate is $k'_{+1}L$, this probability is

$$P = \exp(-k'_{+1}Lt_r) \qquad \text{(A4)}$$

It follows, of course, that the probability of entering the inactive cycle (cycle B in Figure 3) is $1-P$. The average time spent in the inactive cycle must be calculated somewhat differently. As above for the active cycle, the time spent in state M′L is $1/k'_{-1}$. However, the maximal time that can be spent for association of a ligand molecule is t_r, otherwise cycle A is entered. Thus the average time spent for association with the macromolecule M′ is found by integrating only up to time t_r.

$$\int_0^{t_r} tk'_{+1}L\exp(-k'_{+1}Lt_r)\,dt =$$

$$\frac{1}{k'_{+1}L}[1-(1+k'_{+1}Lt_r)\exp(-k'_{+1}Lt_r)] \qquad \text{(A5)}$$

Therefore, the average time spent in the inactive cycle is

$$t(\text{inactive cycle}) =$$

$$\frac{1}{k'_{-1}} + \frac{1}{k'_{+1}L}[1-(1+k'_{+1}Lt_r)\exp(-k'_{+1}Lt_r)] \qquad \text{(A6)}$$

The average time spent in the active state, subsequently called the response R, is obtained by combining eqns. (A2), (A3) and (A6) and weighting these times by the probabilities of passing through the active and inactive cycles:

$$R = \frac{P\left(\frac{1}{k_{-1}}\right)}{P\left(t_r+\frac{1}{k_{+1}L}+\frac{1}{k_{-1}}\right)+(1-P)\left\{\frac{1}{k'_{-1}}+\frac{1}{k'_{+1}L}[1-(1+k'_{+1}Lt_r)\exp(1+k'_{+1}Lt_r)]\right\}} \qquad \text{(A7)}$$

or, as according to eqn. (A4) $P = \exp(-k'_{+1}Lt_r)$, we obtain for the response

$$R = \frac{P\left(\frac{1}{k_{-1}}\right)}{P\left(t_r+\frac{1}{k_{+1}L}+\frac{1}{k_{-1}}\right)+(1-P)\left\{\frac{1}{k'_{-1}}+\frac{1}{k'_{+1}L}[1-(1+k'_{+1}Lt_r)P]\right\}} \qquad \text{(A8)}$$

Several useful normalizations can be applied to reduce the number of free parameters from five (t_r, k_{+1}, k_{-1}, k'_{+1}, k'_{-1}) to three (T, A, B):

$$K_d = \frac{k_{-1}}{k_{+1}}$$

$$K'_d = \frac{k'_{-1}}{k'_{+1}}$$

$$\lambda = \frac{L}{K_d}$$

$$T = k_{-1}t_r = \frac{t_r}{\tau_{occ.}}$$

$$A = \frac{K_d}{K'_d}$$

$$B = \frac{k'_{-1}}{k_{-1}}$$

The response can then be expressed as

$$R = \frac{P\lambda}{P(1+\lambda+\lambda T)+\frac{1-P}{AB}[1+\lambda A-(1+AB\lambda T)P]} \qquad \text{(A9)}$$

In Figure 4 of the main paper, the dose–response curve $D = R(\lambda)$ is dissected into component activation and inhibition curves. The activation curve A is the Langmuir binding isotherm or Michaelis–Menten curve, i.e.

$$\text{Act}(\lambda) = \frac{\lambda}{1+\lambda} \qquad \text{(A10)}$$

An expression for the total inhibition I can be obtained by dividing $R(\lambda)$ by Act (λ):

$$I(\lambda) = \frac{R(\lambda)}{\text{Act}(\lambda)} \qquad \text{(A11)}$$

In Figure 4 of the main paper, the inhibition is subdivided into two components, curves B and C. Curve B represents the inhibition I_B due to the refractory time t_r and is calculated as the amount of inhibition in the absence of a competing pathway (no cycle B in Figure 3). This can be obtained by letting the affinity of M′ for the ligand go to zero, i.e. $K'_d \to \infty$ and $A\ (= K_d/K'_d) \to 0$:

$$I_B(\lambda) = \frac{\text{I}(\lambda, A=0)}{\text{Act}(\lambda)} \qquad \text{(A12)}$$

The remaining inhibition I_C due to the competing pathway (cycle B in Figure 3) is represented by curve C and obtained from

$$I_C(\lambda) = \frac{R(\lambda)}{\mathrm{Act}(\lambda)\, I_B(\lambda)} \tag{A13}$$

The curves in Figures 4 and 5 of the main paper were plotted by computer (program available on request).

As shown in Figure 5 of the main paper, the descending limb of the dose–response curve can be quite steep. Table 2 lists the Hill coefficients (h) that would be necessary to give a Hill-type inhibition of equal steepness. These apparent Hill coefficients were calculated by comparing the maximal steepness of a Hill-type process with the maximal steepness of the inhibition curve $I(\lambda)$ corresponding to eqn. (A11). The maximal steepness of $I(\lambda)$ was calculated numerically. The maximal steepness of a Hill-type inhibition curve was evaluated from

$$I(\lambda)_{\mathrm{Hill}} = \frac{\lambda^h}{1+\lambda^h} \tag{A14}$$

and

$$\frac{\mathrm{d}I(\lambda)_{\mathrm{Hill}}}{\mathrm{d}\ln(\lambda)} = \frac{-h\lambda^h}{(1+\lambda^h)^2} \tag{A15}$$

Eqn. (A15) reaches a maximum when $\lambda = 1$; so

$$\left.\frac{\mathrm{d}I(\lambda)_{\mathrm{Hill}}}{\mathrm{d}\ln(\lambda)}\right|_{\mathrm{max.}} = -\frac{h}{4} \tag{A16}$$

Received 19 May 1993/27 August 1993; accepted 6 September 1993